Accepted Manuscript

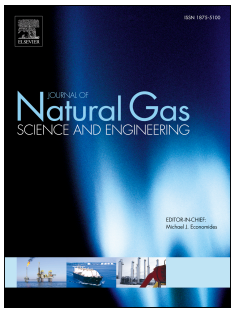

Improving Hole Cleaning using Low Density Polyethylene Beads at Different Mud Circulation Rates in Different Hole Angles

Wong Jenn Yeu, Allan Katende, Farad Sagala, Issham Ismail

PII: S1875-5100(18)30505-5

DOI: https://doi.org/10.1016/j.jngse.2018.11.012

Reference: JNGSE 2764

To appear in: *Journal of Natural Gas Science and Engineering*

Received Date: 30 July 2018

Revised Date: 31 October 2018

Accepted Date: 6 November 2018

Please cite this article as: Yeu, W.J., Katende, A., Sagala, F., Ismail, I., Improving Hole Cleaning using Low Density Polyethylene Beads at Different Mud Circulation Rates in Different Hole Angles, *Journal of Natural Gas Science & Engineering*, https://doi.org/10.1016/j.jngse.2018.11.012.

Improving Hole Cleaning using Low Density Polyethylene Beads at Different Mud Circulation Rates in Different Hole Angles

Wong Jenn Yeu[a], Allan Katende[b,d,*], Farad Sagala[c], Issham Ismail[a]

[a]*Department of Petroleum Engineering,Faculty of Petroleum and Renewable Energy Engineering, Universiti Teknologi Malaysia (UTM), Malaysia.*
[b]*Department of Energy, Minerals and Petroleum Engineering, Faculty of Applied Sciences and Technology, Mbarara University of Science and Technology (MUST), Kihumuro Campus, 7km off Mbarara-Kasese Road, Uganda.*
[c]*Department of Chemical and Petroleum Engineering, University of Calgary (UC), Calgary, Canada*
[d]*Department of Geoscience and Petroleum, Norwegian University of Science and Technology (NTNU), Trondheim, Norway*

Abstract

In oil and gas exploration and development, drilling a hole is one of the first and most expensive operations. The continuous demand from industry to reduce costs and operational problems has resulted in numerous innovative drilling technologies that allow us to drill directionally. Nevertheless, hole cleaning has become a problematic issue in directional drilling because drill cuttings tend to be deposited on the lower side of the deviated hole. Excess accumulation of cuttings significantly reduces the rate of penetration and indirectly increases the operational cost. To improve the cuttings transport efficiency in a deviated hole, low-density polyethylene (LDPE) beads were introduced into water-based mud for hole cleaning. LDPE beads travel rapidly through the mud column due to buoyancy and move the cuttings forward by drag and collision. The interaction between the LDPE beads and cuttings facilitates the cuttings transport process and prevents the cuttings from settling. In this study, different concentrations of LDPE beads (i.e., 1% to 5% by volume) and different flow rates (i.e., 0.4 L/s, 0.6 L/s, and 1.0 L/s) were used to determine the effects on cuttings transport efficiency. In addition, the hole angle was varied from vertical to horizontal to evaluate the significance of LDPE beads in assisting in transporting cuttings. The results denote that more cuttings can be removed from a hole with higher concentrations of LDPE beads in water-based mud. This finding is due to the higher frequency of collisions, which in turn produces larger impulsive force. In addition, the improvement in cuttings transport efficiency enabled by LDPE beads is more significant in a vertical hole than in a highly deviated hole. In summary, LDPE beads are a promising additive for drilling mud to effectively remove drilled cuttings from a hole.

Keywords: Hole Cleaning, Cuttings Lifting Efficiency, LDPE Beads, Water-Based Mud, Hole Angles, Flow Rate

Contents

1.Introduction

Wellbore cleaning is the process of removing cuttings from a hole by fluid circulation during drilling. In directional drilling, the hole is deviated, and cuttings are likely to settle at the bottom of the hole, making hole cleaning difficult. The cuttings environment, which is characterized by annular cuttings concentration and the cuttings bed fraction, is greatly influenced by the wellbore configuration, fluid flow regime, fluid properties, and rate of penetration; Hakim et al. (2018); Khatibi et al. (2018, 2016); Zeng et al. (2018); Majid et al. (2018); Manjula et al. (2017); Kamyab and Rasouli

*Corresponding author
Email address: allan_katende@hotmail.com (Allan Katende)

Received: July 30, 2018; Revised: November 9, 2018

(2016); Sayindla et al. (2017); Song et al. (2017b); Busch et al. (2016); Taghipour et al. (2013); Ji et al. (2010); Duan et al. (2009, 2008); Yu et al. (2004); Cho et al. (2000); Bird and Garrett (1996); Frigaard et al. (1994).

When mud circulation is stopped for drill string replacement, drilling fluids act as a suspension tool to prevent cuttings from settling and filling the hole. The viscosity of the drilling fluid increases as motion slows, enhancing the liquid consistency of the fluid during drilling operations. The drilling fluid then turns into a gel-like substance when drilling has stopped; (Olasunkanmi, 2011; Werner et al., 2017). Cuttings are then suspended within the drilling fluid until the drill string is again inserted or the operation resumes. Then, this gel-like substance transforms back into a liquid when circulation begins again.

Okrajni and Azar (1986) demonstrated that laminar mud flows dominate cuttings flows in low-inclination wells (0^o-45^o), while turbulent mud flows are more favoured in highly deviated wells (55^o–90^o). In 2000, the study by Cho et al. (2000) supported these findings, demonstrating that high-velocity but less-viscous fluid is beneficial for horizontal cuttings transport due to high turbulence. At low inclination angles, suspension is prominent in the cuttings transport process, and therefore, high-viscosity fluid is more favourable; (Sifferman et al., 1974; Bloys et al., 1994). In other words, a viscous fluid is efficient in a nearly vertical segment due to the laminar flow regime, which can prevent particles from settling down and even becoming stuck in the pipe.

Among the factors that influence the cuttings environment (Cho et al., 2000; Ma et al., 2016), fluid rheology and flow rate are the two main factors considered when formulating mud designed for different wellbore conditions to ensure efficient cuttings transport. Fluid rheology is dependent on formation conditions and is important in providing buoyancy to lift and transport cuttings. Moreover, flow rates determine whether the flow pattern is laminar or turbulent; (Kelessidis and Bandelis, 2004). Additives are sometimes added to enhance the performance of drilling fluid and combat borehole problems such as fluid loss and sloughing.

In the cuttings transport process, cuttings are subjected to axial drag forces, upward buoyancy forces and downward gravity. When the net upward force is balanced by the downward force, cuttings tend to settle at a constant rate known as the particle settling velocity; (Sample and Bourgoyne, 1977; Fang, 1992; Song et al., 2017a). Therefore, the drilling mud must flow with an annular velocity that is higher than the cuttings settling velocity.

Pipe rotation and eccentricity also aid in making cuttings transport more efficient in inclined holes than in vertical holes; (Sample and Bourgoyne, 1977; Siginer and Bakhtiyarov, 1998; Nguyen et al., 2010; Walker and Li, 2000; Heydari et al., 2017; Moraveji et al., 2017) because the rotary motion of drilling mud during upward movement can keep the cuttings in suspension for much longer. However, the effect of rotation is more significant in small annulus holes than in large annulus holes; (Ford et al., 1977). When drilling ceases, maintaining pipe rotation prevents cuttings from settling. However, these two parameters were kept constant in this study; i.e., eccentricity is zero because the drill pipe is located at the centre of a large pipe. In our study, we assume that the drilling activity is halted temporarily but that mud circulation must continue to prevent barite and cuttings, among other species, from settling to bottom–hole.

In a deviated hole, the distribution of cuttings in the annulus is asymmetric and greatly depends on the hole inclination. In the nearly-horizontal segment, the fluid column can be described by three layers, namely, the stationary bed (non-moving cuttings) at the bottom, the moving bed (flowing cuttings) above the stationary bed, and a heterogeneous suspension (cuttings-free fluid) on top, as shown in Figure 1. Turbulence in the suspended layer can shear bed cuttings and lift them for removal. Below a well deviation of 60^o, the cuttings bed begins to disappear and diminishes at approximately 30^o; (Tom, 1987; Luo et al., 1994; Hyun et al., 2000; Salem and El-Din, 2006; Ozbayoglu et al., 2010; Akhshik et al., 2018; Ernesto et al., 2016; Zeng et al., 2018; Epelle and Gerogiorgis, 2018) .

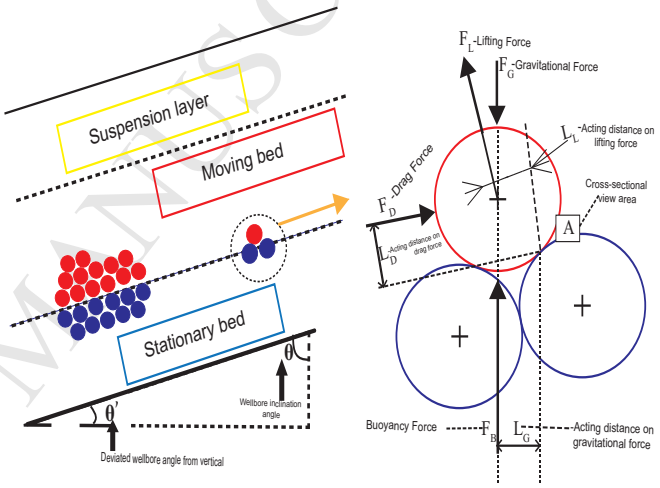

Figure 1: Schematic diagrams of horizontal segment and forces acting on particles at the lower stratum of moving bed.(Hyun et al., 2000)

In the nearly vertical segment, the stationary bed is non-existent, and cuttings transport is dominated by in situ axial velocity; i.e., a sufficient axial velocity of the circulating fluid is necessary to maintain the drilled cuttings in suspension for longer. However, the axial velocity of fluid decreases with increasing wellbore deviation. Thus, it is more difficult to clean deviated holes than vertical holes due to the existence of the stationary bed and low axial velocity.

Yi et al. (2017) performed experiments on cuttings lifting efficiency using low- and high-density polyethylene beads in different hole angles. Their experiments used a mud formulation from Scomi (2018) without commercial viscosifiers in order to better observe the effect of polymer beads on hole cleaning. Their results revealed that both types of beads (low- and high-density polyethylene) improve hole cleaning efficiency better than basic mud. However, the low-density polyethylene beads performed better than high-density polyethylene beads.

Hakim et al. (2018) investigated the performance of polyethylene and polypropylene beads in drill cuttings transportation in a horizontal wellbore. Their analysis involved using a mud formulation from Scomi (2018) in order to ob-

serve the effect of polymer beads on hole cleaning. Cuttings transport efficiency (CTE) was measured for polyethylene and polypropylene Beads with cuttings sizes ranging from 0.5 mm to 4.00 mm while keeping the rig fixed in only the horizontal position. The results showed that polymer beads improved the hole cleaning efficiency but also that polypropylene beads performed better than polyethylene beads.

In this study, low-density polyethylene (LDPE) beads (7.7 ppg) were introduced based on the findings from; Yi et al. (2017) and Hakim et al. (2018) to not only improve mud lubricity but also aid in cuttings transport at different bead concentrations, hole angles and mud flow rates. Table 1 shows the comparison of previous studies using polymer beads for cuttings transport and the major focus of our study. LDPE beads are chemically inert and not reactive with water. Most importantly, the beads are less dense than WBM. Therefore, LDPE beads travel faster through the mud column due to buoyancy and collide with and push the cuttings in the flow direction. However, LDPE beads reduce the overall mud density, and therefore, the addition of barite is needed to achieve the target mud weight. They also have a high melting point of 450^{o}C which makes them suitable to be used when drilling in a high temperature hole.

Table 1: Comparison between previous studies using polymer beads for cuttings transport and the focus of this study

Item	**Yi et al. (2017)**	**Hakim et al. (2018)**	**Concentration of our study.**
Focus of the study	• Used low density PE (LDPE) beads and high density PE (HDPE) beads in water-based mud. • The PE beads were selected because they have a higher melting temperature > 400$^o F$, which is suitable to be used in high temperature holes as well.	• Polyethylene (PE) beads and polypropylene (PP) beads were used in water-based mud.	• Used LDPE beads in water-based mud because they perform better than HDPE beads. • Extended the study of Yi et al. (2017) and Hakim et al. (2018).
Scope	• Looked into the Horizontal (90^o) hole angle only.	• Looked into the Vertical(0^o), 60^o and Horizontal (90^o) hole angles.	• Looked into more hole angles to determine the most critical angle. • Hole angles studied included, the Vertical(0^o),45^o, 60^o and Horizontal (90^o) hole angles. • Tested variable mud flow rates.
Rheological properties, fluid loss and rheological model	• Tested and reported	• Tested and reported	• Tested and reported
Dynamic test variables	1. Different holes angles: Vertical(0^o), 60^o and Horizontal (90^o) hole angles. 2. Different concentrations of LDPE and HDPE beads (0% to 5%) by volume.	1. Different cuttings sizes 2. Different concentrations of PE and PP beads (0% to 5%) by volume.	• Studied more variables on cuttings transport ratio performance in water-based mud which include: 1. Covered more holes angles to be the most critical angle: the Vertical(0^o),45^o, 60^o and Horizontal (90^o) hole angles. 2. Different concentrations of LDPE beads (0% to 5%) by volume. 3. Different mud flow rates: 0.4 l/s, 0.6 l/s, and 1.0 l/s.

2.Experimental Set-Up and Methods

2.1.Drilling Mud Preparation

Prior to the simulated hole cleaning, WBM samples with and without LDPE beads were prepared, the rheological properties of these samples were determined. LDPE beads were prepared in five different concentrations by volume and added to the WBM.

To formulate the mud, 350 ml of tap water was added to 15 g of bentonite, 1.0 g of starch, and 0.25 g of soda ash. Next, the LDPE beads were added into the mud in volumetric concentrations. Lastly, barite was added to increase the mud density to 10 ppg.

Different concentrations (by volume) of LDPE beads were used in the experiment, namely, 1%, 2%, 3%, 4% and 5%, as shown in Table 2. The amount or weight of LDPE beads in volumetric concentrations can be determined from their density.

Table 2: Composition of WBM with LDPE beads

Mud Sample No.	Mud compositions in lab scale
1	350 ml water + 15g bentonite + 1 g starch + 0.25 g soda ash + 145 g barite
2	350 ml water + 15g bentonite + 1 g starch + 0.25 g soda ash + 151 g barite + 1% v/v LDPE
3	350 ml water + 15g bentonite + 1 g starch + 0.25 g soda ash + 158 g barite + 2% v/v LDPE
4	350 ml water + 15g bentonite + 1 g starch + 0.25 g soda ash + 163 g barite + 3% v/v LDPE
5	350 ml water + 15g bentonite + 1 g starch + 0.25 g soda ash + 171 g barite + 4% v/v LDPE
6	350 ml water + 15g bentonite + 1 g starch + 0.25 g soda ash + 176 g barite + 5% v/v LDPE

2.1.1.Mud Rheological Properties Measurement

A 400 ml basic water-based mud sample was prepared to measure its mud weight, plastic viscosity, gel strength, and yield point. The mud preparation was done using a mud mixer. Its density and rheological properties were measured using a mud balance and rheometer, respectively. The same procedures were used for the water-based mud sample with LDPE beads.

2.2.Materials Properties

2.2.1.Sand Cuttings

To simulate the drilled cuttings inside the wellbore, sand particles with sizes ranging between 1.18 mm and 2.00 mm were added to the drilling fluid to circulate in the cuttings lifting flow loop.

In the preparation of the sand samples, the sand particles were washed, cleaned and dried in the typical laboratory oven shown in Figure 2(a) . After that, the sieve shaker shown in Figure 2(b) was used to sieve the sand samples in order to obtain the desired size between 1.18 mm and 2.00 mm.

(a) Laboratory Oven

(b) Sieve Shaker.

Figure 2: Laboratory equipment used in preparation of sand cuttings.

Figure 3: Simulated drilled cuttings in separated bags.

Next, the sieved sand samples were weighed using an electronic balance, and 200 g of the sand was sealed in each transparent plastic bag, as shown in Figure 3.

The density of the sand particles was determined by computation as shown in Section 2.2.1.1.

2.2.1.1 Density of Sand Cuttings

Using the sand replacement method, the masses of both dry sand and wet sand were measured in a container to calculate the density of sand. The data obtained are presented in Table 3.

Table 3: Density calculations for sand cuttings

Mass of beaker	3.46 g
Volume of beaker	95.00 cc
Mass of beaker + dry sand	159.00 g
Mass of beaker + wet sand	195.60 g
Sand porosity = $\frac{(195.6-159)g}{(1g/cc \times 95cc)}$	**0.3853**
Mass of dry sand	155.54 g
Volume of dry sand = 95 cc x (1-0.3853)	58.40 cc
Density of sand	**2.66 g/cc**

2.2.2.Density of LDPE Beads

Figure 4: LDPE beads

The LDPE beads of a 4-mm (0.16") nominal granule size shown in Figure 4 were used in this study. The density of the LDPE beads was pre-determined by the water displacement method in order to facilitate the experimental calculations, as shown in Table 4. The results showed that the beads have a density of 0.92/cc, which is less than that of the drilling mud.

Table 4: LDPE bead density calculations

Mass of cylinder + 20 ml water	146.2 g
Mass of cylinder + 20 ml water +10 ml LDPE beads	155.4 g
Mass of LDPE bead	9.2 g
Volume of LDPE beads	10 ml
Density of LDPE beads	**0.92 g/cc**

LDPE beads can be applied in the field, as bit nozzles with sizes in the range from 6.35 mm (0.25 inch) to 25.4 mm (1 inch) are available.

To prepare the desired water-based mud samples with LDPE beads, the concentration of LDPE beads was varied from 1.0 to 5.0% by volume. The LDPE beads have a melting point temperature of 450^{o}C, which enables them to be used in drilling high-temperature holes. They are chemically inert and do not react with the components in water-based mud. Details of their properties are given in Table 5.

Table 5: Properties of LDPE beads

Properties	**Titanlene LDi300yy**	**ASTM method**
Melt index (g/10 min)	20	D1238
Melting point (^{o}C)	450	D1238
Density (g/cm^3)	0.92	D1505
Vicat softening point (^{o}C)	87	D1525
Tensile strength at yield (kg/cm^2)	120	D638
Tensile strength at break (kg/cm^2)	100	D638
Elongation at break (%)	120	D638
1% Secant modulus (kg/cm^2)	1900	D638
Low-temperature brittleness (^{o}C)	-35	D746

2.2.3.Analysis of the LDPE Beads

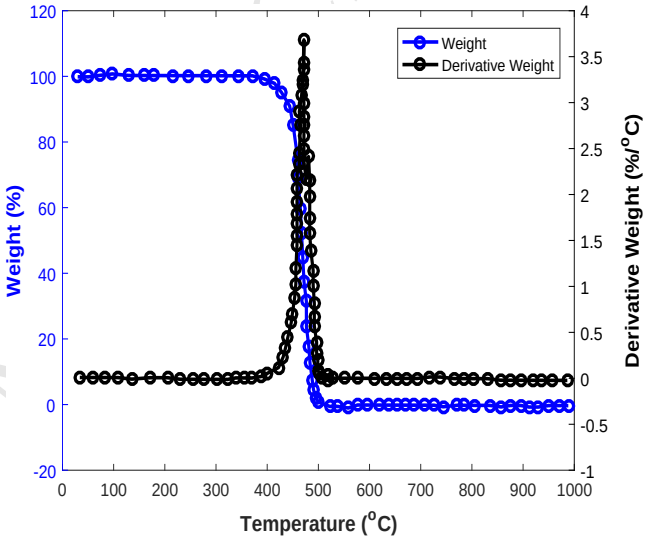

Figure 5: TGA results for LDPE beads

LDPE beads were examined using thermogravimetric analysis[1] (TGA) in order to characterize them and to observe changes in their physical properties with increasing temperature. The change in the weight of the LDPE beads was measured as the temperature increased, as shown in Figure 5. In addition, the derivative weight loss curve indicates that the maximum weight loss occurred at 450.41^{o}C, which is the melting point of the beads.

2.3.Experimental Set-up

The lab-scale flow loop was designed to demonstrate the effect of pipe angles on cuttings transport through the simulator rig. Before the experimental work was conducted, the lab-scale flow loop was tested several times to ensure that each section could function smoothly and thus that the data obtained would be reliable. The layout and schematic diagram of the flow loop are shown in Figures 6(a) and 6(b), respectively.

[1]This method measures weight change as a result of temperature change

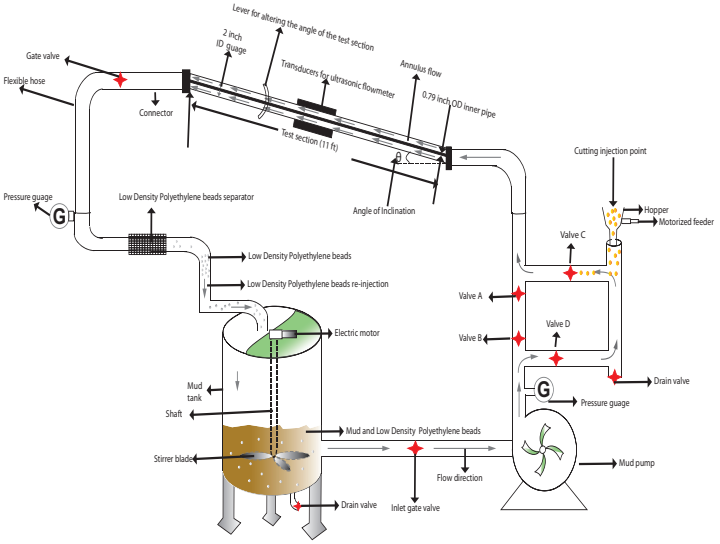

(a) Schematic of the flow loop rig simulator.

(b) Layout of the flow loop rig simulator.

Figure 6: Flow loop rig simulator.

2.3.1.Annular Test Section

Figure 7: Annular test section.

The annular test section shown in Figure 7 consists of a 11-ft-long transparent acrylic outer pipe (50 mm OD and 45.6 mm ID) and a hollow PVC inner pipe (12.6 mm OD). The inner pipe was sealed at both ends to prevent mud from flowing within. Then, the inner pipe was installed inside an acrylic pipe with a support every 4 ft to maintain concentricity throughout the test section. There was no rotation for the inner pipe throughout the experiment. The test section was designed to be capable of being rotated to any angle from vertical to horizontal to represent a deviated hole.

2.3.2.Experimental Procedure

The experiment was conducted using the lab-scale flow loop at ambient temperature and pressure. The test procedure was designed specifically to investigate the improvement of cuttings transport efficiency using WBM with LDPE beads in a deviated hole. Throughout the experiment, the pipe angle, mud flow rate and concentrations of LDPE beads were the varying parameters, while all the other parameters, such as the drilling mud density and pipe eccentricity, were kept constant.

Prior to initiating the experimental work, the entire flow loop was flushed with clear water for 10 minutes to eliminate any impurities from the flow lines. For the first stage of the experiment, 80 litres of basic water-based mud sample (without LDPE beads) with a density of 10 ppg was prepared in the mud tank and circulated at 0.4 L/s in the vertical annuli (0^o angle) at ambient temperature for half an hour to achieve a homogeneous state. This process was performed by opening valves A and B while keeping valves C and D closed to isolate the cuttings feed hopper, as illustrated in Figure 6(a). Once a constant flow velocity of mud, which was monitored using an ultrasonic flow meter, was achieved in the line, the sieved sand particles were injected into the flow system through the cuttings feed hopper. The end cap should be tightly sealed after the introduction of the sand particles. Once the experimental work began, valve A was closed, and valves C and D were opened to divert the mud flow in order to flush the sand particles. Each test was allowed to run for 6 minutes. The transported sand particles were collected, washed, dried, and weighed to obtain the mass of sand that was lifted across the test section, which indicates the cuttings carrying capacity of the mud. After completion of the run, the entire flow loop was flushed again with clear water to clean the flow loop and remove the remaining sand or impurities from the system. To obtain a data point, three test runs were done prior to taking/calculating an average value in order to ensure consistency. The steps were repeated for another four angles of annuli, namely, 30^o, 45^o, 60^o, and 90^o horizontal annuli, and two flow rates of 0.6 L/s and 1.0 L/s.

For the second stage of the experiment, LDPE beads were introduced into the 80 litres of basic water-based mud sample with a density of 10 ppg via the polymer feed hopper one minute after the injection of the sand particles. Flow in the system was achieved by opening valves B, C, and D while

keeping valve A closed. The sieve at the system outlet was selected so that it would trap LDPE beads but permit sand particles to be collected separately. Each test run was conducted for 6 minutes. The lifted sands were washed, dried, and weighed to determine the cuttings transport ratio. After completion of the run, the entire flow loop was flushed again with clear water to clean the flow loop and remove the remaining sand or impurities from the system. To obtain a data point, three test runs were done prior to taking/calculating an average value in order to ensure consistency. The steps were performed for all five angles of annuli, namely, 0^o, 30^o, 45^o, 60^o, and 90^o; three flow rates of 0.4 L/s, 0.6 L/s and 1.0 L/s; and five LDPE beads concentrations of 1.0, 2.0, 3.0, 4.0, and 5.0% (by volume).

3.Results and Discussions

3.1.Drilling Mud Rheology

WBM with and without LDPE beads was prepared at the lab scale with compositions as shown in Table 2. The rheological properties of the mud before and after the ageing process were tested, and the results are shown in Table 6 and Table 7.

Table 6: Mud rheological properties before ageing

Drilling mud	**Rheological properties (before ageing)**						
	ρ **(ppg)**	μ_a **(cp)**	μ_p **(cp)**	**YP (lb/100ft^2)**	**GS (lb/100ft^2) 10 s-10 m**	**FL (ml)**	**MCT (/32in)**
WBM	10	9	7	5	3-8	10	2.31
WBM+1% LDPE	10	9	7	5	3-8	11.2	2.53
WBM+2% LDPE	10	9	7	5	3-8	14.2	2.7
WBM+3% LDPE	10	9	7	5	3-8	15.2	2.95
WBM+4% LDPE	10	9	7	5	3-8	15.4	3.3
WBM+5% LDPE	10	9	7	5	3-8	16	3.62

Table 7: Mud rheological properties after ageing

Drilling mud	**Rheological properties (after ageing)**						
	ρ **(ppg)**	μ_a **(cp)**	μ_p **(cp)**	**YP (lb/100ft^2)**	**GS (lb/100ft^2) 10 s-10 m**	**FL (ml)**	**MCT (/32in)**
WBM	10	21	15	26	8–25	17.8	2.3
WBM+1% LDPE	10	21	15	26	8–25	17.8	2.9
WBM+2% LDPE	10	21	15	26	8–25	16.8	3.38
WBM+3% LDPE	10	21	15	26	8–25	16.2	3.72
WBM+4% LDPE	10	21	15	26	8–25	15	4.29
WBM+5% LDPE	10	21	15	26	8–25	14.4	4.6

The drilling mud samples were also subjected to high pressure and high temperature (HPHT) conditions as shown in Table 8 to determine the fluid losses. The pressure and temperature used were 500 psig and 250 ^{o}F, respectively.

Table 8: Fluid loss of drilling mud under HPHT

Drilling mud	HPHT	
	FL (ml)	MCT (/32in)
WBM	35	10.9
WBM+1% LDPE	32.5	11.26
WBM+2% LDPE	30.4	12.7
WBM+3% LDPE	28.9	13.7
WBM+4% LDPE	26.4	15.37
WBM+5% LDPE	25	16.3

3.2.Cuttings Transport Ratio (CTR)

In the experiment, the pipe angle was varied from vertical to horizontal to determine the effect of hole inclinations on the CTR of drilling mud. The concentration of LDPE beads in drilling mud was also varied to investigate the extent of the improvement in CTR. Furthermore, the flow rate was varied to study the performance of both drilling mud and LDPE beads in different flow regimes.

3.2.1.Effect of the Hole Angle

In the experiment, the pipe angle was set at 0^o (vertical), 30^o, 45^o, 60^o and 90^o (horizontal). Figure 8 illustrates the effect of hole inclinations on hole cleaning. In each curve, the CTR of basic WBM is plotted against the hole angles for different flow rates. These results also served as the baseline values for the subsequent experiments to examine the effects of LDPE beads on CTR.

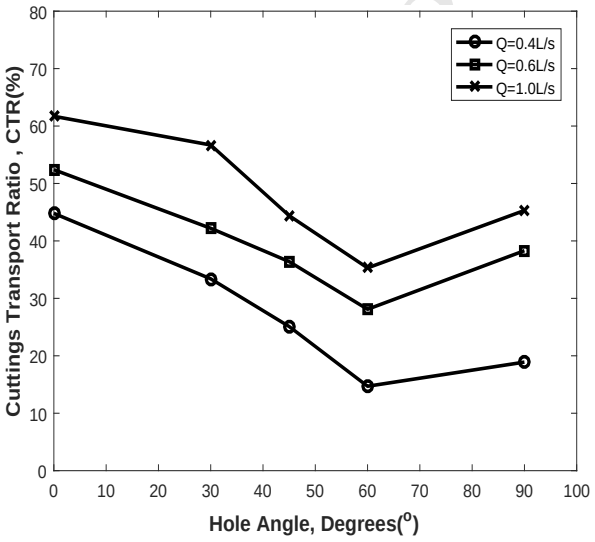

Figure 8: Cuttings transport ratio versus hole inclination for basic WBM

At all angles, the CTR of drilling mud increased with increasing flow rate. This result indicates that higher annular velocities can clear away more drilled cuttings. The highest CTRs for each flow rate was found in vertical holes with values of 62% at 1.0 L/s, 52% at 0.6 L/s and 45% at 0.4 L/s. This result is because all the drag forces provided by mud flow translated to lift when parallel with gravity, that is, the resultant lift is the highest in a vertical hole. Next, the CTR at a 30^o inclination was found to be the second highest, and such wells are considered to be low-inclination wells, as indicated by; Okrajni and Azar (1986).

The lowest CTRs occurred at 60^o inclination with values of 15% at 0.4 L/s, 28% at 0.6 L/s and 35% at 1.0 L/s. This result is because the force of lift, which dominates cuttings transport, is greatly reduced by the high inclination. The resultant force against gravity is lower, and hence, drilled cuttings tend to settle downward.

The second-lowest CTR was found at 45^o inclination, and the worst was found in horizontal holes, with values of 0.6 L/s and 1.0 L/s, respectively. However, at 0.4 L/s, corresponding to laminar flow, the second-worst CTR was found in the horizontal well, followed by the well with a 45^o inclination. Compared to the hole angle with the worst CTR, 60^o, the horizontal well exhibited better cuttings transport because the dominant force was axial drag force, which was not affected by inclination, and thus, the cuttings would not slip backward. In addition, the drag force is increased by higher flow rates.

3.2.2.Effect of Flow Rate

Three flow rates, namely, 0.4 L/s, 0.6 L/s and 1.0 L/s, were used to develop laminar, transition and nearly turbulent flows, respectively. As shown in Figure 9, higher flow rates increased CTR due to the production of turbulent eddies.

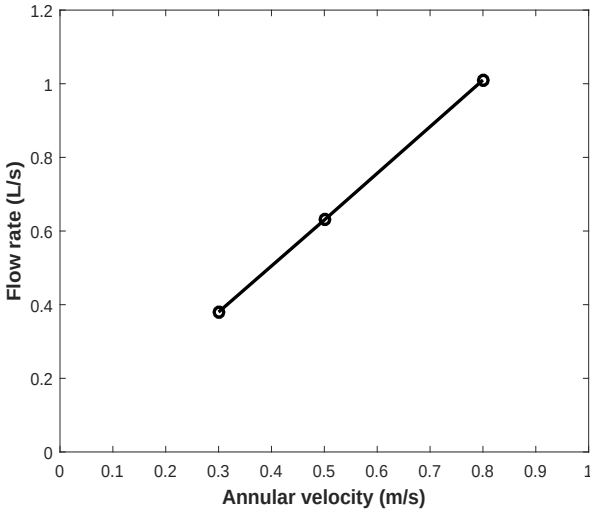

Figure 9: Flow rate relative to annular velocities used in the experiment.

3.2.3.Force Analysis

LDPE beads were added to drilling mud with the purpose of transporting more cuttings from the wellbore to the surface. As discussed, two types of force are involved in this mechanism, namely, buoyancy force and impulsive force.

1. Buoyancy Force

   Based on Equation A8 in Appendix A.4, the buoyancy force generated by LDPE beads is directly proportional to the volume of the beads. However, the volume

of each bead used in the experiment was assumed to be the same with a diameter of 3 mm. Hence, at certain angles, the buoyancy force produced by the LDPE beads was the same regardless of the concentration of beads.

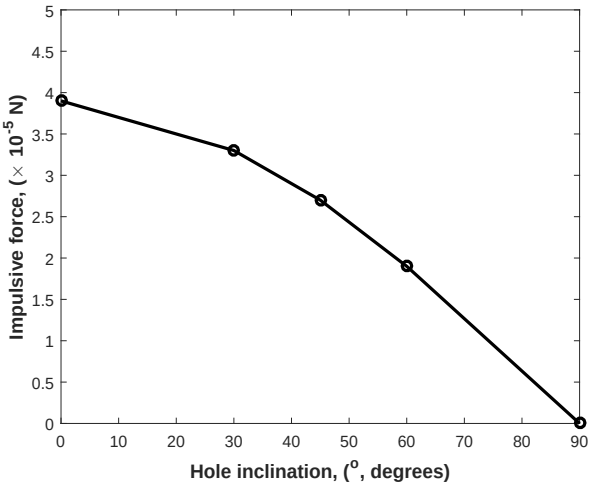

Figure 10: The impulsive force produced by LDPE beads at different hole inclinations

The upward buoyancy force enables LDPE beads to travel with higher velocity in the mud flow stream. The calculations for buoyancy force are shown in Table A.5 in Appendix A.4. However, the resultant force in the mud flow direction diminished at higher hole inclinations approaching the horizontal, as shown in Figure 10. This result indicated that the significance of the buoyancy force provided by LDPE beads and the improvement in CTR decreased in highly deviated holes.

2. Impulsive Force

High-velocity LDPE beads collided with the sand cuttings and produced impulsive force that accelerated the cuttings upward. The calculations for the impulsive force between beads and cuttings are shown in Table A.6 in Appendix A.5. Figure 11 shows that impulsive force increases with higher concentrations of LDPE beads. This result is because more beads increase the frequency of collision.

The impulsive force decreased with higher hole inclinations, as shown in Figure 12. The collisions between beads and sand cuttings is the lowest in the horizontal hole because the velocities of the beads and cuttings are almost the same. Second, due to their low density, the LDPE beads tend to float on top of the horizontal hole, and hence, the collision rate is near zero.

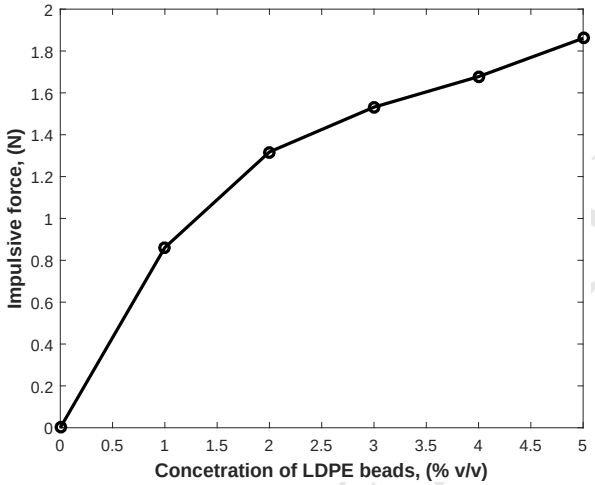

Figure 11: Impulsive force versus concentration of LDPE beads in a vertical hole at 1.0 L/s.

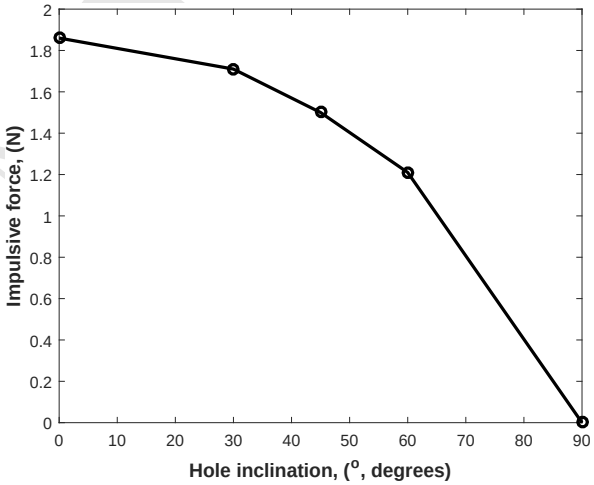

Figure 12: Impulsive force at 5% v/v LDPE beads versus hole inclination at 1.0 L/s

3.2.4.Effect of Concentration of LDPE Beads

LDPE beads were added into WBM at concentrations of 1%, 2%, 3%, 4% and 5% by volume. At different hole angles, the improvement of CTR by LDPE beads was observed and plotted as a function of the concentration of beads.

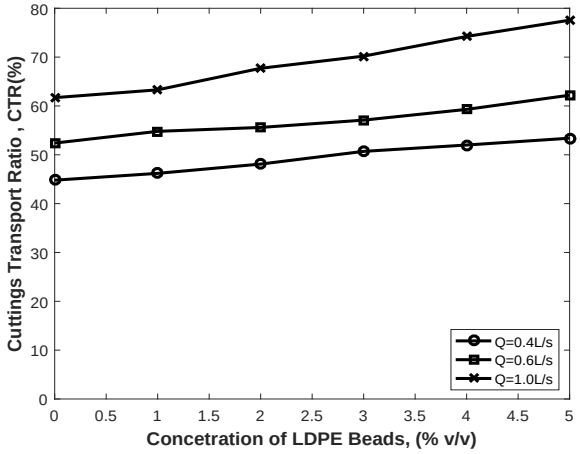

Figure 13: CTR versus concentrations of LDPE beads in a vertical hole for different flow rates.

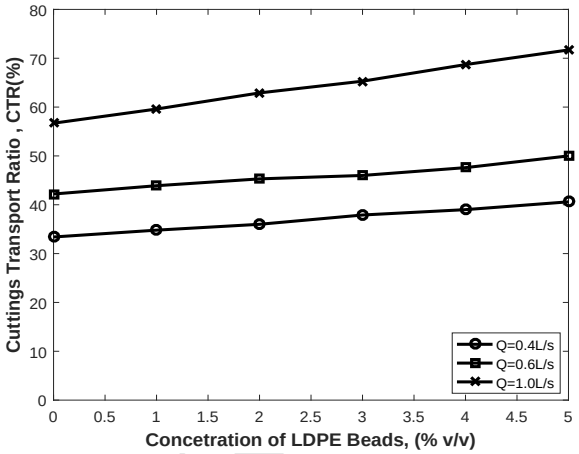

Figure 14: CTR versus concentrations of LDPE beads at a 30^o hole inclination for different flow rates

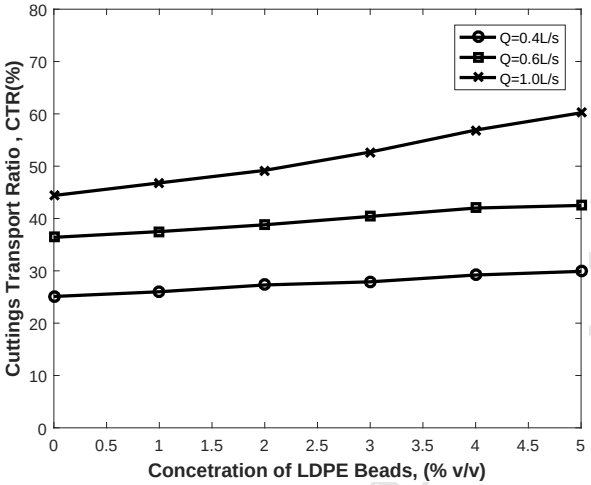

Figure 15: CTR versus concentrations of LDPE beads at 45^o hole inclination for different flow rates.

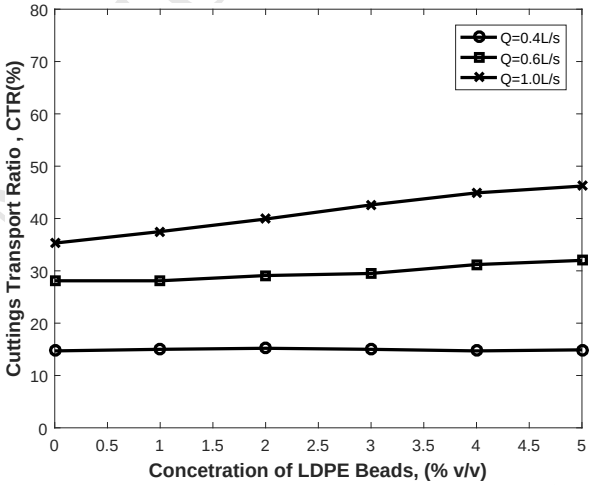

Figure 16: CTR versus concentrations of LDPE beads at a 60^o hole inclination for different flow rates

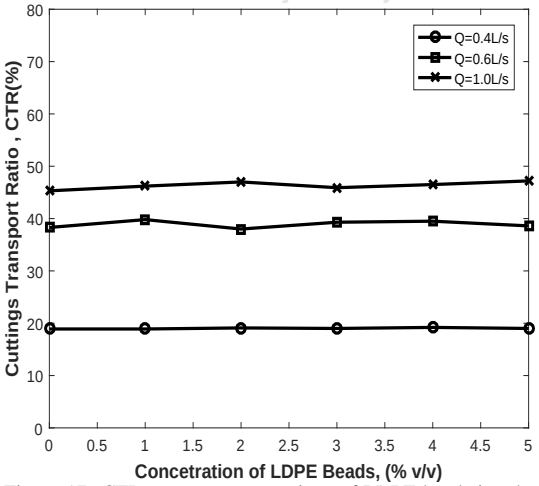

Figure 17: CTR versus concentrations of LDPE beads in a horizontal hole for different flow rates.

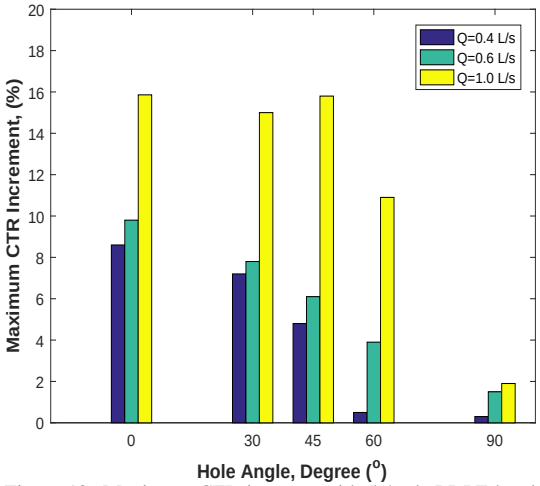

Figure 18: Maximum CTR increase with 5% v/v LDPE beads at different hole inclinations and different flow rates

From the graphs above (Figures 13, 14, 15, 16, 17, 18), the greater the concentration of LDPE beads used in drilling mud is, the higher the CTR in the hole. In short, a 5% v/v concentration of LDPE beads resulted in the highest CTR. This result implied that the impulsive force generated by the beads helped to lift drilled cuttings efficiently to the surface.

The change in CTR in WBM with 5% v/v LDPE beads at each hole inclination was calculated and is presented in Figure 16. The results clearly illustrate that LDPE beads in the vertical hole resulted in the greatest CTR values of 8.6%, 9.8% and 15.9% at 0.4 L/s, 0.6 L/s and 1.0 L/s. At higher flow rates, the impulse generated by LDPE beads on cuttings was higher, and hence, more cuttings were transported.

The results also showed that CTR decreased with higher hole inclinations because the beads tend to float on top of the hole. Therefore, the performance of LDPE beads was the poorest in horizontal well with CTR values of less than 1.3%.

4.Conclusions

This research focused on the improvement in CTR using LDPE beads in WBM. To achieve this objective, a wellbore cleaning system was designed and constructed. Two important alterable variables in drilling operations, namely, hole inclination and circulation rate, were chosen as the focuses of this study. The important findings from this study can be summarized as follows:

1. Among the hole inclinations, the 90^o(horizontal hole) was the worst angle for wellbore cleaning, followed by the hole with an inclination of 60^o. This result is because the resultant force due to hole inclination is lower, and the cuttings tend to accumulate at the bottom of the hole and slip downward for the hole with a 60^o inclination. For the 90^o hole, beads were found to float at the top of the horizontal section. In contrast, the vertical hole showed the best CTR due to low accumulation of cuttings. Hole cleaning is thus more difficult in a deviated hole than in a vertical hole.
2. The flow rate significantly affected the CTR. The higher the flow rate was, the higher the annular velocity, and the higher the CTE. This result is because higher annular velocities generate higher axial forces to push the cuttings. In addition, the turbidity of the flow stream also promoted an even distribution of cuttings inside the hole. This even distribution greatly reduced the accumulation of cuttings to one side of the hole. Turbulent flow is expected to produce the best hole cleaning, but turbulent flows are limited by hydraulic availability in field. Therefore, a transition flow was used in the experiment and showed a positive result in hole cleaning.
3. The addition of LDPE beads improved the CTR by maximum of 15.9%. The beads travelled faster through the mud column due to the buoyancy force and collided with sand cuttings, imparting an impulsive force that moved the cuttings forward. A greater concentration of LDPE beads resulted in more effective hole cleaning. The CTR was the lowest in the horizontal well because the beads were not able to collide with cuttings when floating. However, at higher flow rates, the effects of the LDPE beads were magnified, and the CTR was higher. This result is due to the even distribution of beads and cuttings, which induced a higher impulsive force.

5.Nomenclature

a	Acceleration
CTR	Cuttings transport ratio
F_b	Buoyancy force
F_{imp}	Impulsive force
F_{net}	Resultant force
F_d	Drag force
F_L	Lifting force
FL	Fluid loss
GS	Gel strength
hp	Horse power
Q	Flow rate
L_G	Acting distance on gravitational force
L_D	Acting distance on drag force
L_L	Acting distance on lifting force
LDPE	Low-density polyethylene
L/s	Litres per second
m	Mass
MCT	Mud cake thickness
rpm	Revolutions per minute
t	time
TGA	Thermogravimetric analysis
v	Velocity
A	Cross-sectional area
A_{an}	Annular area
τ	Shear stress
R_e	Reynolds number
ASTM	American Section of the International Association for Testing Materials
HPHT	High pressure high temperature
W_f	Weight of collected sand cuttings
W_i	Initial weight of sand cuttings
V_p	Volume of LDPE bead
W	Weight
WBM	Water-based mud
YP	Yield strength
θ	Inclination
ρ	Density
ρ_p	Density of LDPE bead
μ_a	Apparent viscosity
μ_p	Plastic viscosity
d_c	Cuttings diameter
d_1	Inner pipe diameter
d_2	Annular diameter
ρ_c	Cuttings density
ρ_f	Drilling fluid density
v_s	Settling velocity of cuttings
v_{an}	Annular velocity

Competing Interests.

The authors declare no competing interests

Bibliography

S. Akhshik, M. Behzad, and M. Rajabi. CFD-DEM simulation of the hole cleaning process in a deviated well drilling: The effects of particle shape. *Particuology*, 25:72–82, 2018. doi: https://doi.org/10.1016/j.partic.2015.02.008.

J. J. Azar and G. R. Samuel. *Drilling Engineering*. PennWell Corp, 2007. ISBN 1-59370-072-5,978-1-59370-072-0. Pages 171–187.

J. Bird and C. Garrett. Co-polymer Beads Reduce Friction In Horizontal Wells. pages 1–4. Society of Petroleum Engineers, Journal of Canadian Petroleum Technology, September 1996. doi: https://doi.org/10.2118/96-09-GE.

B. Bloys, N. Davis, B. Smolen, L. Bailey, L. Fraser, and M. Hodder. Annular Velocity For Rotary Drilling Operations. *Oilfield Review–Schlumberger*, 6(2):33–43, 1994. doi: https://www.slb.com/~/media/Files/resources/oilfield_review/ors94/0494/p33_43.pdf.

A. Busch, A. Islam, D. Martins, F. P. Iversen, M. Khatibi, S. T. Johansen, R. W. Time, and E. A. Meese. Cuttings Transport Modeling - Part 1: Specification of Benchmark Parameters with a Norwegian Continental Shelf Perspective. pages 1–32. Society of Petroleum Engineers, SPE Bergen One Day Seminar, 20 April, Grieghallen, Bergen, Norway, 2016. doi: https://doi.org/10.2118/180007-MS.

S.-F. Chien. Annular Velocity For Rotary Drilling Operations. *International Journal of Rock Mechanics and Mining Sciences & Geomechanics Abstracts*, 9(3):403–416, 1972. doi: https://doi.org/10.1016/0148-9062(72)90005-8.

H. Cho, S. N. Shah, and S. O. Osisanya. A Three-Layer Modeling for Cuttings Transport with Coiled Tubing Horizontal Drilling. pages 1–14. Society of Petroleum Engineers, SPE Annual Technical Conference and Exhibition, 1-4 October, Dallas, Texas, 2000. doi: https://doi.org/10.2118/63269-MS.

M. Duan, S. Z. Miska, M. Yu, N. E. Takach, R. M. Ahmed, and C. M. Zettner. Transport of Small Cuttings in Extended-Reach Drilling. pages 1–8. Society of Petroleum Engineers, SPE Journal, September 2008. doi: https://doi.org/10.2118/104192-PA.

M. Duan, S. Z. Miska, M. Yu, N. E. Takach, R. M. Ahmed, and C. M. Zettner. Critical Conditions for Effective Sand-Sized Solids Transport in Horizontal and High-Angle Wells. pages 1–10. Society of Petroleum Engineers, SPE Journal, June 2009. doi: https://doi.org/10.2118/106707-PA.

E. I. Epelle and D. I. Gerogiorgis. CFD modelling and simulation of drill cuttings transport efficiency in annular bends: Effect of particle sphericity. *Journal of Petroleum Science and Engineering*, 170:992–1004, 2018. doi: https://doi.org/10.1016/j.petrol.2018.06.041.

F. Ernesto, R. Corredor, M. Bizhani, and E. Kuru. Experimental investigation of cuttings bed erosion in horizontal wells using water and drag reducing fluids . *Journal of Petroleum Science and Engineering*, 147:129–142, 2016. doi: https://doi.org/10.1016/j.petrol.2016.05.013.

G. Fang. An Experimental Study Of Free Settling Of Cuttings In Newtonian And Non-Newtonian Drillings Fluids: Drag Coefficient And Settling Velocity. pages 1–11. Society of Petroleum Engineers, 1992 Society of Petroleum Engineers, 1992. doi: https://www.onepetro.org/general/SPE-26125-MS.

J. Ford, J. Peden, M. Oyeneyin, E. Gao, and R. Zarrough. An Experimental Evaluation Of Correlations Used For Predicting Cutting Slip Velocity. pages 1–12. Society of Petroleum Engineers, SPE Annual Fall Technical Conference and Exhibition, 9-12 October, Denver, Colorado, 1977. doi: https://doi.org/10.2118/6645-MS.

I. A. Frigaard, S. D. Howison, and I. J. Sobey. On the stability of Poiseuille flow of a Bingham fluid. *Journal of Fluid Mechanics*, 263(25):133–150, 1994. doi: https://doi.org/10.1017/S0022112094004052.

H. Hakim, A. Katende, F. Sagala, I. Ismail, and H. Nsamba. Performance of polyethylene and polypropylene beads towards drill cuttings transportation in horizontal wellbore. *Journal of Petroleum Science and Engineering*, 165:962–969, 2018. doi: https://doi.org/10.1016/j.petrol.2018.01.075.

O. Heydari, E. Sahraei, and P. Skalle. Investigating the impact of drillpipe's rotation and eccentricity on cuttings transport phenomenon in various horizontal annuluses using computational fluid dynamics (CFD) . *Journal of Petroleum Science and Engineering*, 156:801–813, 2017. doi: https://doi.org/10.1016/j.petrol.2017.06.059.

C. Hyun, N. S. Subhash, and S. O. Osisanya. A Three-Segment Hydraulic Model for Cuttings Transport in Horizontal and Deviated Wells. pages 1–14. Society of Petroleum Engineers, SPE/CIM International Conference on Horizontal Well Technology, 6-8 November, Calgary, Alberta, Canada, 2000. doi: https://doi.org/10.2118/65488-MS.

L. Ji, Q. Guo, and C. Wang. Is It Possible to Inject Larger Sizes and Higher Solids Concentrations of Drill Cuttings? pages 1–10. Society of Petroleum Engineers, International Oil and Gas Conference and Exhibition in China, 8-10 June, Beijing, China, 2010. doi: https://doi.org/10.2118/131347-MS.

M. Kamyab and V. Rasouli. Experimental and numerical simulation of cuttings transportation in coiled tubing drilling. *Journal of Natural Gas Science and Engineering*, 29:284–302, 2016. doi: https://doi.org/10.1016/j.jngse.2015.11.022.

V. Kelessidis and G. Bandelis. Flow Patterns and Minimum Suspension Velocity for Efficient Cuttings Transport in Horizontal and Deviated Wells in Coiled-Tubing Drilling. pages 1–15. Society of Petroleum Engineers, SPE Drilling and Completion, 2004. doi: https://doi.org/10.2118/81746-PA.

M. Khatibi, R. W. Time, and H. A. Rabenjafimanantsoa. Particles falling through viscoelastic non-Newtonian flows in a horizontal rectangular channel analyzed with PIV and PTV techniques. *Journal of Non-Newtonian Fluid Mechanics*, 235:143–153, 2016. doi: https://doi.org/10.1016/j.jnnfm.2016.08.004.

M. Khatibi, R. W. Time, and R. Shaibu. Dynamical feature of particle dunes in Newtonian and shear-thinning flows: Relevance to hole-cleaning in pipe and annulus. *International Journal of Multiphase Flow*, 99:284–293, 2018. doi: https://doi.org/10.1016/j.ijmultiphaseflow.2017.10.015.

Y. Luo, P. Bern, and B. Chambers. Simple Charts To Determine Hole Cleaning Requirements in Deviated Wells. pages 1–7. Society of Petroleum Engineers, SPE/IADC Drilling Conference, 15-18 February, Dallas, Texas, 1994. doi: https://doi.org/10.2118/27486-MS.

T. Ma, P. Chen, and J. Zhao. Overview on vertical and directional drilling technologies for the exploration and exploitation of deep petroleum resources. *Geomechanics and Geophysics for Geo-Energy and Geo-Resources*, 2(4):365–395, 2016. doi: https://link.springer.com/content/pdf/10.1007%2Fs40948-016-0038-y.pdf.

N. F. F. Majid, A. Katende, I. Ismail, F. Sagala, N. M. Sharif, and M. A. C. Yunus. A comprehensive investigation on the performance of durian rind as a lost circulation material in water based drilling mud. *Petroleum*, 2018. doi: https://doi.org/10.1016/j.petlm.2018.10.004.

E. V. P. J. Manjula, W. K. H. Ariyaratne, C. Ratnayake, and M. C. Melaaena. A review of CFD modelling studies on pneumatic conveying and challenges in modelling offshore drill cuttings transport . *Powder Technology*, 329:782–793, 2017. doi: https://doi.org/10.1016/j.powtec.2016.10.026.

M. K. Moraveji, M. S. A. Shahryari, and A. Ghaffarkhah. Investigation of drill pipe rotation effect on cutting transport with aerated mud using CFD approach. *Advanced Powder Technology*, 28:1141–1153, 2017. doi: https://doi.org/10.1016/j.apt.2017.01.020.

T. N. Nguyen, S. Z. Miska, M. Yu, N. E. Takach, and R. Ahmed. Experimental study of hydraulic sweeps in horizontal wells. *International Oil-Gas AGH Conference*, 2010. doi: http://yadda.icm.edu.pl/baztech/element/bwmeta1.element.baztech-article-AGHM-0024-0028/c/Nguyen.pdf.

S. Okrajni and J. Azar. The Effects of Mud Rheology on Annular Hole Cleaning in Directional Wells. pages 1–12. Society of Petroleum Engineers, SPE Drilling Engineering, 1986. doi: https://doi.org/10.2118/14178-PA.

A. M. Olasunkanmi. *Graphical Evaluation of Cuttings Transport in Deviated Wells using Bingham Plastic Fluid Model*. PhD thesis, African University of Science and Technology, Abuja, Nigeria, November 2011. URL http://repository.ngren.edu.ng:8080/handle/123456789/10667.

M. E. Ozbayoglu, A. Saasen, M. Sorgun, and K. Svanes. Critical Fluid Velocities for Removing Cuttings Bed Inside Horizontal and Deviated Wells. *Petroleum Science and Technology*, 28(6):594–602, 2010. doi: https://doi.org/10.1080/10916460903070181.

S. E. Salem and M. N. El-Din. Drillpipe Eccentricity Prediction During Drilling Directional Wells. pages 1–6. Petroleum Society of Canada, Canadian International Petroleum Conference, 13-15 June, Calgary, Alberta, 2006. doi: https://doi.org/10.2118/2006-047.

K. Sample and A. Bourgoyne. An Experimental Evaluation Of Correlations Used For Predicting Cutting Slip Velocity. pages 1–12. Society of Petroleum Engineers, SPE Annual Fall Technical Conference and Exhibition, 9-12 October, Denver, Colorado, 1977. doi: https://doi.org/10.2118/6645-MS.

S. Sayindla, B. Lund, J. D. Ytrehus, and A. Saasen. Hole-cleaning performance comparison of oil-based and water-based drilling fluids. *Journal of Petroleum Science and Engineering*, 159:49–57, 2017. doi: https://doi.org/10.1016/j.petrol.2017.08.069.

Scomi. Drilling Fluids. http://www.scomigroup.com.my/GUI/pdf/drilling_fluid.pdf, 2018. [Online; Last accessed 19-MArch-2018].

T. R. Sifferman, G. M. Myers, E. L. Haden, and H. A. Wahl. Drill cutting

transport in full scale vertical annuli. *Journal of Petroleum Technology*, 26:1295–1302, 1974. doi: https://doi.org/10.2118/4514-PA.

D. A. Siginer and S. I. Bakhtiyarov. Flow of drilling fluids in eccentric annuli. *Journal of Non-Newtonian Fluid Mechanics*, 78(2-3):119–132, 1998. doi: https://doi.org/10.1016/S0377-0257(97)00101-8.

P. Skalle. *Drilling Fluid Engineering*. BookBoon, 2010. ISBN 9788776815523. Pages 66–100.

X. Song, Z. Xu, G. Li, Z. Pang, and Z. Zhu. A new model for predicting drag coefficient and settling velocity of spherical and non-spherical particle in Newtonian fluid . *Powder Technology*, 321:242–250, 2017a. doi: https://doi.org/10.1016/j.powtec.2017.08.017.

X. Song, Z. Xu, M. Wang, G. Li, S. N. Shah, and Z. Pang. Experimental Study on the Wellbore-Cleaning Efficiency of Microhole-Horizontal-Well Drilling. pages 1–12. Society of Petroleum Engineers, SPE Journal, August 2017b. doi: https://doi.org/10.2118/185965-PA.

A. Taghipour, B. rnar Lund, J. D. Ytrehus, P. l Skalle, A. Saasen, A. Reyes, and J. Abdollahi. Experimental Study of Hydraulics and Cuttings Transport in Circular and Non-Circular Wellbores. *Journal of Energy Resources Technology*, 136:1–9, 2013. doi: https://doi.org/10.1115/OMAE2013-11317.

I. Tom. *Directional Drilling*. Petroleum Engineering and Development Studies. Springer, 1987. ISBN ISBN 978-94-017-1270-5.

S. Walker and J. Li. The Effects of Particle Size, Fluid Rheology, and Pipe Eccentricity on Cuttings Transport. pages 1–10. Society of Petroleum Engineers, SPE/ICoTA Coiled Tubing Roundtable, 5-6 April, Houston, Texas, 2000. doi: https://doi.org/10.2118/60755-MS.

B. Werner, V. Myrseth, and A. Saasen. Viscoelastic properties of drilling fluids and their influence on cuttings transport. *Journal of Petroleum Science and Engineering*, 156:845–851, 2017. doi: https://doi.org/10.1016/j.petrol.2017.06.063.

T. T. Yi, I. Ismail, A. Katende, F. Sagala, and J. Mugisa. Experimental Investigation of Cuttings Lifting Efficiency Using Low and High Density Polyethylene Beads in Different Hole Angles. *Journal of Materials Sciences and Applications*, 3(5):71–78, 2017. doi: http://article.aascit.org/file/pdf/8910898.pdf.

M. Yu, D. Melcher, N. Takach, S. Z. Miska, and R. Ahmed. A New Approach to Improve Cuttings Transport in Horizontal and Inclined Wells . pages 1–8. Society of Petroleum Engineers, SPE Journal, September 2004. doi: https://doi.org/10.2118/90529-MS.

C. Zeng, X. Yan, Z. Zeng, and S. Yang. The formation and broken of cuttings bed during reaming process in horizontal directional drilling. *Tunnelling and Underground Space Technology*, 76:21–29, 2018. doi: https://doi.org/10.1016/j.tust.2018.03.008.

Appendix A. Wellbore Cleaning Calculations

A.1.Annular Flow of Drilling Mud

Hole dimensions; $d_1 = 1.80$ in
$d_2 = 0.85$ in

Annular Area:

$$A_{an} = \frac{\pi(1.8^2 - 0.85^2)}{4 \times 144} = 13.73 \times 10^{-3} ft^2$$

Flow rate:

$$Q = AnnularArea \times AnnularVelocity \quad \text{(A1)}$$

Reynolds number was calculated using the following equation;

$$Re = \frac{928 \rho v_a d_e}{\mu} \quad \text{(A2)}$$

Where; $d_e = (d_1 - d_2)$ and $\mu = \frac{\tau}{\gamma}$
Mud weight = 10ppg and Viscosity = 7cp

Table A.1: Experimental annular velocities and flow rates for drilling mud

Re	Annular velocity		Flow rate
1250	0.30 m/s	1.0 ft/s	0.38 L/s
2130	0.52 m/s	1.7 ft/s	0.63 L/s
3390	0.82 m/s	2.7 ft/s	1.01 L/s

A.2.Settling Velocities of Cuttings

$\mu = 7$cp
$\rho_f = 10$-ppg
$\rho_c = 12.7$-ppg
$d_c = 0.063$-in

$$\frac{\mu}{\rho_f \times d_c} = 11.1$$

According to Chien (1972), if $\frac{\mu}{\rho_f \times d_c} > 10$, then Equation A3 must be used to determine velocity of the cuttings as follows:

$$v_s = 0.45 \left(\frac{\mu}{\rho_f \times d_c}\right) \left[\sqrt{\frac{36,800}{\left(\frac{\mu}{\rho_f \times d_c}\right)^2} \times d_c \left(\frac{\rho_c}{\rho_f} - 1\right) + 1} - 1 \right] \quad \text{(A3)}$$

Hence;

$$v_s = 0.45\,(11.1) \left[\sqrt{\frac{36,800}{(11.1)^2} \times 0.063 \left(\frac{12.7}{10} - 1\right) + 1} - 1 \right]$$
$$= 7.32 ft/min \quad or \quad 0.12 ft/s$$

The net velocity of cuttings transport is obtained from Equation A4 as follows:

$$v_t = v_{an} - v_s \quad \text{(A4)}$$

Table A.2: Cuttings transport velocity at different flow rates in a vertical hole

Flow rate	v_{an}	v_s	v_t
0.4 L/s	1.0 ft/s	0.12 ft/s	0.88 ft/s
0.6 L/s	1.7 ft/s	0.12 ft/s	1.58 ft/s
1.0 L/s	2.7 ft/s	0.12 ft/s	2.58 ft/s

A.3.Experimental Calculations for the LDPE Beads

The volumetric concentration of LDPE beads was calculated based on the volume of the test section (11 feet long).

Volume of the test section = $13.73 \times 10^{-3} ft^2 \times 11 ft$
$= 0.151 ft^3$

Knowing the volume of test section and density of LDPE beads, the number of LDPE beads for each concentration in the hole cleaning experiment was calculated as follows:

Beads Volume = Test Section Volume × Concentration.
Beads Mass = Beads Volume × 0.92 g/cc

Table A.3: Amount of LDPE beads required for the wellbore cleaning experiment

Concentration	Injected LDPE beads	
	Volume (cc)	Mass (g)
1%	43	39
2%	86	79
3%	128	118
4%	171	157
5%	214	197

The LDPE beads are sieved out with the cuttings throughout the experiment. Therefore, the same amount of beads must be injected back into the drilling mud in every minute of the experiment. The collected beads are also weighed to determine the flow rate of the beads.

Table A.4: Amount of LDPE beads required for re-injection and the beads flow rate.

Concentration	Collected beads After 1 minute (g)	Beads flow rate (g/s)
1%	33	0.55
2%	59	0.98
3%	78	1.3
4%	96	1.6
5%	118	1.97

A.3.0.1 Mode of Calculation and Assumptions

The mode of calculation in Appendix A.4 & A.5 is based on one LDPE bead using the concept of buoyancy and impulsive forces.

The following assumptions are made;

1. Effect of hole temperature on LDPE bead is neglected
2. Mud properties do not change
3. Constant mud density

4. LDPE bead does collide with other LDPE bead
5. LDPE bead completely submerges in mud
6. Slippage velocity is neglected
7. Effect of shear stress and shear strain is neglected

The limitations taken into consideration include the following;

1. Mud properties deteriorate over time
2. LDPE bead has tendency to stick to another LDPE bead
3. Flow regime may change

A.4.Buoyancy Force

Based on Archimedes' principle (Azar and Samuel, 2007; Skalle, 2010), when a less dense object is partially or wholly immersed in a denser medium (fluid), an upward force will be exerted by the fluid in opposition to the weight of the immersed object, W, as shown in Figure A.1

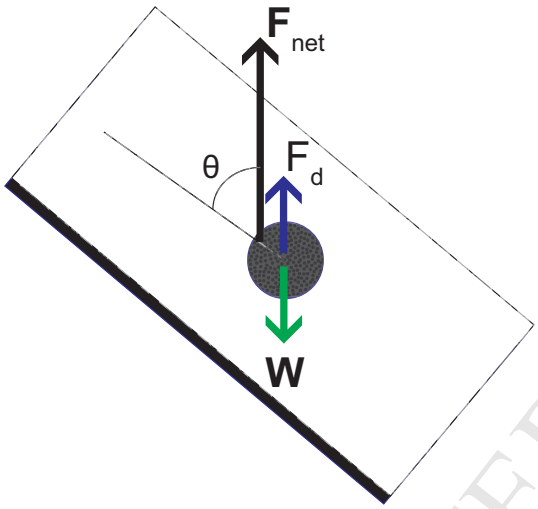

Figure A.1: Buoyancy force on an immersed LDPE bead or cutting

For a less dense object given that;

$$F_b = \rho_f \cdot g \cdot V_p \tag{A5}$$

$$W = \rho_p \cdot g \cdot V_p \tag{A6}$$

$$F_{net} = F_b - W = g \cdot V_p \cdot \left(\rho_f - \rho_p\right) \tag{A7}$$

$$F_{axial} = F_{net} \cdot cos(\theta) \rightarrow For \quad inclined \quad holes \tag{A8}$$

Therefore, the acceleration of LDPE beads in a drilling fluid is given by the following;

$$m \cdot a = g \cdot V_p \cdot \left(\rho_f - \rho_p\right) \cdot cos(\theta)$$

$$\therefore a = \frac{g \cdot V_p \cdot \left(\rho_f - \rho_p\right) \cdot cos(\theta)}{m} \equiv \frac{g \cdot \cancel{V_p} \cdot \left(\rho_f - \rho_p\right) \cdot cos(\theta)}{\cancel{V_p} \cdot \rho_p}$$

$$\therefore a = \frac{g \cdot \left(\rho_f - \rho_p\right) \cdot cos(\theta)}{\rho_p} \tag{A9}$$

The resultant force due to buoyancy aided in transporting cuttings to the surface. The magnitude of this force is directly proportional to the difference in density between the polyethylene beads and the mud. Second, as the wellbore deviation increases, the force generated in the axial direction to move cuttings gradually diminishes.

LDPE beads have a lower density than drilling mud, and hence, the beads generate buoyancy, thus travelling faster and aiding in transporting cuttings. Equation A8 showed that the magnitude of the buoyancy force is directly proportional to bead volume and inversely proportional to hole inclination. Buoyancy force is independent of the concentration of LDPE beads. The resultant buoyant force parallel to the stream flow in different hole inclinations is calculated using Equation A8 and is presented in Table A.5 below.

$$Volume \quad of \quad beads = \frac{4}{3 \times 8}\pi\left(3 \times 10^{-3} m\right)^3 = 1.414 \times 10^{-8} m^3 \tag{A10}$$

$$Buoyancy \quad force, F_b = (9.81)\left(1.14 \times 10^{-3}\right)(1198 - 920) = 0.039 \times 10^{-3} N \quad in \quad the \quad upward \quad direction$$

Table A.5: Buoyancy force by LDPE beads in different hole inclinations

Hole inclination	0^o	30^o	45^o	60^o	90^o
Buoyancy force ($\times 10^{-5}$ N)	3.9	3.3	2.7	1.9	0

A.5.Impulsive Force

Impulsive force (Azar and Samuel, 2007; Skalle, 2010), was imparted as the PE beads collided with sand cuttings, causing the cuttings to move forward. Therefore, a change in momentum is involved. Some assumptions are made to facilitate the calculations, including the following:

1. Initially, sand cuttings travel at v_t, while PE beads travel at the mud flow velocity, v_{an}.
2. Both the beads and cuttings travel together with same velocity after collision.
3. The time elapsed for impulse is equivalent to the time required for all injected beads to flow through the test section. This time can be obtained as follows:

$$Time = \frac{(Amount \quad of \quad injected \quad beads)}{(Beads \quad Flow \quad Rate)} \tag{A11}$$

4. The impulsive force is the lowest when the beads travel at the initial velocity, which is the same as the mud flow velocity. The impulsive force was greatest at the end of the test section as the beads travel at the fastest speed after acceleration due to the buoyancy force.

For example, for the 1% v/v concentration of LDPE beads in a vertical hole with a 0.8m/s annular velocity, the following calculations were conducted. The amount of injected beads and beads flow rate are 39 g and 0.55 g/s, respectively, as obtained from Tables A.3 and A.4.

Beads Velocity

Initial Velocity, $v_1 = 0.8$ m/s

Acceleration, a = $9.81\left(\frac{1198-920}{920}\right)\times\cos(0^o) = 2.96 m/s^2$

Maximum Velocity, $v_{max} = \sqrt{v_1^2 + 2as}$

$= \sqrt{0.8^2 + 2(2.96)(3.35)} = 4.52 m/s$

Maximum Velocity, $v_{mean} = \frac{v_1+v_{max}}{2} = 2.66 m/s$

Change in Momentum

$$m_p v_p + m_c v_c = \left(m_p + m_c\right) v_f$$

$m_p = 39g$, $m_c = 200g$, $v_c = v_t = 0.79 m/s$, $v_p = 2.66 m/s$.

$$\therefore v_f = \frac{(39\times2.66+200\times0.79)}{(39+200)} = 1.10 m/s$$

Impulsive Force

$$F = \frac{(m\times\Delta v)}{t}$$

Where $t = \frac{(39g)}{(0.55g/s)}$

$$\therefore F = \frac{39\times(1.10-2.66)}{71} = -0.86N$$

The force is negative as the force is imparted to the beads themselves after collision, thus slowing the beads down. At the same time, this same amount of force is imposed on the sand particles, causing them to move faster. These dynamics are consistent with Newtons Third Law of Motion.

The magnitude of impulsive force is directly proportional to the mass of the beads and the change in velocity. Therefore, as the concentration of beads increased, a larger impulsive force was generated to move the cuttings forward.

In addition, the more deviated the well is, the lower the buoyancy force and velocity of beads are, resulting in a smaller impulsive force.

Table A.6: Impulsive force at different concentrations of LDPE beads flowing in a vertical hole at 1.0 L/s

Concentration	Impulsive force (N)				
	0^o	30^o	45^o	60^o	90^o
1%	-0.86	-0.79	-0.7	-0.56	0
2%	-1.32	-1.21	-1.06	-0.85	0
3%	-1.53	-1.41	-1.24	-0.99	0
4%	-1.67	-1.54	-1.35	-1.09	0
5%	-1.86	-1.71	-1.5	-1.21	0

A.6.Cuttings Transport Ratio (CTR)

After the sand particles were collected, dried and weighed, the CTR was calculated using Equation A12 below.

$$CTR = \frac{Weight\ \ of\ \ Transported\ \ Cuttings}{Weight\ \ of\ \ all\ \ Cuttings} \times 100\% = \frac{W_f}{W_i} \times 100\% \quad \text{(A12)}$$

Table A.7: Cuttings transport ratio for all drilling mud types at 0.4 L/s

Mud type	Cuttings transport ratio (0.4 L/s)				
	0^o	30^o	45^o	60^o	90^o
WBM	45%	33%	25%	15%	19%
WBM + 1% v/v LDPE	46%	35%	26%	15%	19%
WBM + 2% v/v LDPE	48%	36%	27%	15%	19%
WBM + 3% v/v LDPE	51%	38%	28%	15%	19%
WBM + 4% v/v LDPE	52%	39%	29%	15%	19%
WBM + 5% v/v LDPE	53%	41%	30%	15%	19%

Table A.8: Cuttings transport ratio for all drilling mud types at 0.6 L/s

Mud type	Cuttings transport ratio (0.6 L/s)				
	0^o	30^o	45^o	60^o	90^o
WBM	52%	42%	36%	28%	38%
WBM + 1% v/v LDPE	55%	44%	38%	28%	40%
WBM + 2% v/v LDPE	56%	45%	39%	29%	38%
WBM + 3% v/v LDPE	57%	46%	40%	30%	39%
WBM + 4% v/v LDPE	59%	48%	42%	31%	40%
WBM + 5% v/v LDPE	62%	50%	43%	32%	39%

Table A.9: Cuttings transport ratio for all drilling mud types at 1.0 L/s

Mud type	Cuttings transport ratio (1.0L/s)				
	0^o	30^o	45^o	60^o	90^o
WBM	62%	57%	44%	35%	45%
WBM + 1% v/v LDPE	63%	60%	47%	38%	46%
WBM + 2% v/v LDPE	68%	63%	49%	40%	47%
WBM + 3% v/v LDPE	70%	65%	53%	43%	46%
WBM + 4% v/v LDPE	74%	69%	57%	45%	47%
WBM + 5% v/v LDPE	78%	72%	60%	46%	47%